

# Modelling the mid-late Holocene evolution of the Huelva Estuary and its human colonization, South-Western Spain

Luis M. Cáceres<sup>a,\*</sup>, Paula Gómez<sup>a</sup>, María L. González-Regalado<sup>a</sup>, María J. Clemente<sup>a</sup>, Joaquín Rodríguez-Vidal<sup>a</sup>, Antonio Toscano<sup>a</sup>, Guadalupe Monge<sup>b</sup>, Manuel Abad<sup>c</sup>, Tatiana Izquierdo<sup>c</sup>, Antonio M. Monge Soares<sup>d</sup>, Francisco Ruiz<sup>a</sup>, Juan M. Campos<sup>e</sup>, Javier Bermejo<sup>e</sup>, Aranzazu Martínez-Aguirre<sup>f</sup>, Gloria I. López<sup>g</sup>

<sup>a</sup> Departamento de Ciencias de la Tierra, Universidad de Huelva, Avda. Tres de Marzo s/n, 21071 Huelva, Spain

<sup>b</sup> Departamento de Cristalografía, Mineralogía y Química Agrícola, Universidad de Sevilla, 41071 Sevilla, Spain

<sup>c</sup> Vicerrectoría de Investigación, Universidad de Atacama, Avda. Copayapu 485, Copiapó, Chile

<sup>d</sup> Centro de Ciências e Tecnologias Nucleares (C<sup>2</sup>TN), Instituto Superior Técnico, Universidade de Lisboa, Estrada Nacional 10 (k 139.7), 2695-066 Bobadela LRS, Portugal

<sup>e</sup> Departamento de Historia I, Universidad de Huelva, Avda. Tres de Marzo s/n, 21071 Huelva, Spain

<sup>f</sup> Departamento de Física Aplicada I, EUITA, Universidad de Sevilla, Crta. Utrera km 1, 41013 Sevilla, Spain

<sup>g</sup> Centro Nacional de Investigación sobre la Evolución Humana, Paseo Sierra de Atapuerca 3, 09002 Burgos, Spain

## ABSTRACT

### Keywords:

Mid-late Holocene  
Palaeogeography  
Huelva Estuary  
SW Spain  
Radiocarbon dating  
Tempestite

The major changes that occurred in the southwestern estuaries of the Spanish Atlantic coast during the last 6500 yr BP were simultaneous to human settlement and therefore the understanding of their coastal evolution will help interpreting human patterns in these areas. The study of the morpho-sedimentary features of new outcrops appearing in the middle sector of Saltés Island (Huelva Estuary, Spain) has been used to develop a model to understand the complex evolution of sand barriers than can be applied to similar inlets along the Atlantic Iberian coast.

The first human settlements (6000–4000 yr BP) in the early Huelva Estuary (Tinto and Odiel rivers) were located in the ancient coastal banks or in the nearby hills. From 4000 yr BP onwards, the estuarine sediments started to emerge as sand barriers and chenier plains, prograding towards the mouth. As the littoral strands stabilized morphologically, they were colonized by human settlements in successive periods, the oldest inland (Almendral) and more recent outward (Cascajera). The study of the upper sedimentary layers of La Cascajera barrier display a tempestitic sequence of landward progradational washover-fans. The calibrated and modelled AMS dates in marine shells provide a storminess time range between the second half of first century BCE and the entire first century CE.

Sedimentary records are useful to evaluate environmental changes, either from natural or anthropogenic causes, such as global and climate change. The interrelationship between the archaeological findings (mainly salting fish factories and old ports) and the morpho-sedimentary evolution at the mouth of the Tinto and Odiel rivers allows us to highlight not only the Huelva Estuary's dynamics evolution, but also the possible regional patterns of human habitation from the beginning of the present sea-level highstand (middle Holocene).

## 1. Introduction

The confluence of the Tinto and Odiel rivers constitutes the *Marismas del Odiel* Natural Park (Fig. 1) and it represents an excellent example of a mid-late Holocene sedimentary infill system of a discrete tidal estuary known as the Huelva Estuary (southwestern of Spain, Western Europe). Many coastal changes have occurred after the last

Postglacial sea-level highstand, including the stabilization of the coastal dynamics and the terrestrial environmental changes affecting run-off and sediment transport (c.f. Borrego et al., 1993; Zazo et al., 1994; Morales, 1997; Goy et al., 2003; among others). The coastal plain and near-shore environments offer a very dynamic geochronology which holds the key evidence to better understand the relationships between marine and terrestrial records. The studied geochronologies include lagoonal,

\* Corresponding author.

E-mail address: [mcaceres@uhu.es](mailto:mcaceres@uhu.es) (L.M. Cáceres).

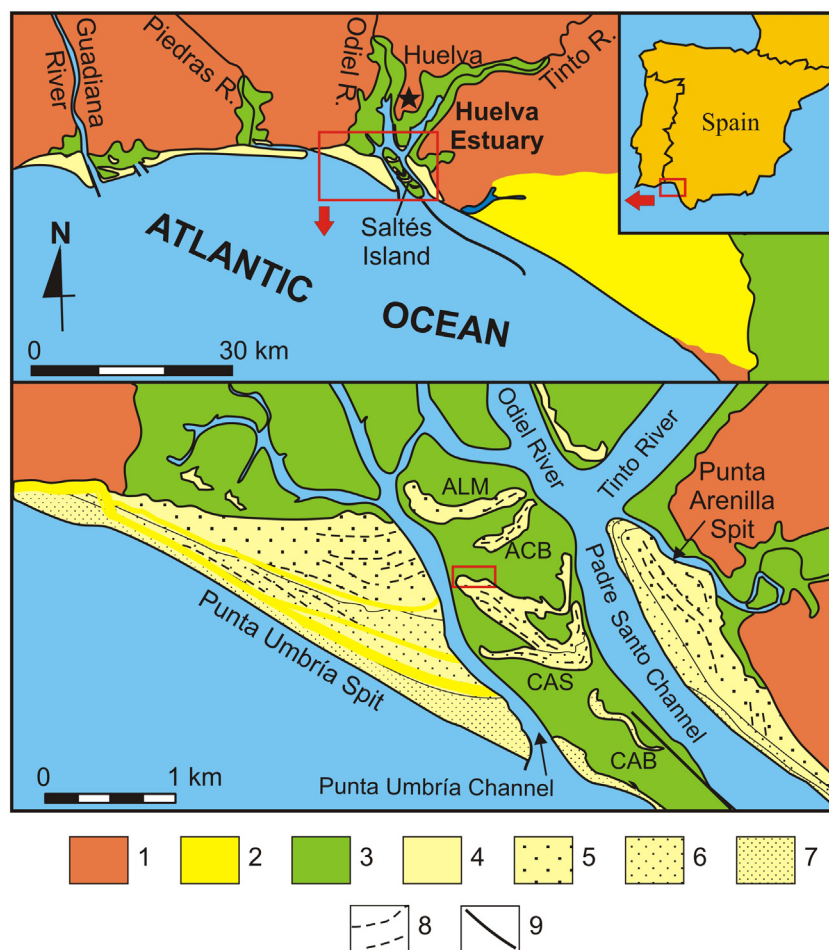


**Fig. 1.** Geographical setting of the Huelva Estuary, showing both Tinto and Odiel rivers and Saltés Island. Sandy barriers in Saltés Island: ALM, El Almendral; ACB, El Acebuchar; CAS, La Cascajera; CAB, Cabezo Alto. The third red rectangle is the location of the Fig. 2. Key: 1. Pre-Holocene substrate, 2. aeolian units, 3. marshland, 4. sand barrier and spits (general), 5. H<sub>2</sub> unit of sand barrier and spits progradation, 6. H<sub>3</sub> unit, 7. H<sub>4</sub> unit, 8. beach ridges, 9. jetty. (For interpretation of the references to colour in this figure legend, the reader is referred to the web version of this article.)

aeolian, intertidal and marine sediments preserved within a diversity of geomorphic features including dunes, spit-barriers, back-barriers and estuaries. On the other hand, as many significant archaeological sites are placed in coastal locations, understanding the land-sea interaction is key to better comprehend human settlement patterns (c.f. Campos et al., 1999, 2002; Alonso et al., 2007, 2009; Silva et al., 2009; Rodríguez-Vidal et al., 2011, 2014; Grützner et al., 2012; among others).

In this context, the Holocene geological record of littoral areas has experienced an increasing multi-disciplinary research over the last decades. Thus, there has been considerable improvement in the knowledge related to the evolution of these environments including sea-level changes (at the regional and global scale), palaeoclimatology and the human settlement pattern vs environment interaction (Borrego et al., 2004; Vilanova et al., 2006; Selby and Smith, 2007). This has favoured the continuous development of coastal geoarchaeology in many countries. However, geomorphological, sedimentological and palaeoenvironmental approaches in these types of geoarchaeological studies frequently lack the integration of archaeological and historical data (Rodríguez-Vidal et al., 2015). This work aims to provide a multi-disciplinary platform to define the relationship between the coastal environmental evolution and human settlement patterns in the Huelva Estuary since the mid to late Holocene, as an example of strategic research approach for other Atlantic Iberian estuaries along the Gulf of Cádiz.

## 2. Study area

### 2.1. Physiographic and geomorphological setting

The Huelva Estuary is located in the central sector of the South Iberian Atlantic coast (Fig. 1). Nowadays this estuary is completely filled with sediments and has started to prograde to build a delta (Morales et al., 2014). This silting has resulted in the development of either tidal flats with salt marshes along the edges of the estuary or islands inside the estuary. The largest of these islands, named Saltés Island, is located on the outer area of the estuary between Punta Umbría and Punta Arenillas spits (Fig. 1), isolated from the mainland by Punta Umbría tidal channel and Padre Santo channel, the main outlets of the Tinto and Odiel rivers. Saltés is the only island in the estuary that contains isolated remains of past sand barrier systems that abruptly contrast with the surrounding muddy marshlands. These sandy systems are, from N to S: El Almendral, El Acebuchal, La Cascajera and Cabezo Alto. This investigation focuses on the northwest edge of the largest sand barrier, La Cascajera, where well exposed stratigraphic sequences were identified.

The origin of these sandy formations is still an issue as different interpretations have been proposed. Initially, Rodríguez-Vidal (1987) proposed a rapid growth model for these estuarine sand barriers as a consequence of the advancement of Punta Umbría spit towards the E and SE, by littoral drift, and the subsequent development of sand hooks sheltering marsh and tidal flats. The erosive action of the 218–209 BCE

tsunami (Ruiz et al., 2013), also evidenced in the Guadalquivir Estuary (Rodríguez-Vidal et al., 2011), and subsequent littoral drift action would have caused the development of sandy beaches attached to the southeast edge of the spit and the present configuration of Saltés Island. Later, Borrego et al. (2000) found similarities between Saltés Island and other chenier plains with differences regarding the wave-energy conditions of formation. Thus, they suggested that Saltés Island should have also behaved as a chenier plain, at least during the last 200 years.

More recently, Morales et al. (2014) proposed a new evolutionary model based on the development of a tidal flat and coalescent sand bars that migrate inland, formed at ebb-tidal deltas shelter. In this sense, Rodríguez-Vidal et al. (2014) relates the sand bars of Saltés Island with chenier plains, with a vertical sand accumulation product of superimposed storm deposits, and their inland progradation as a result of progressive accretion caused by washover fans. This vertical accretionary process could be rapid, as in La Cascajera where the sand bar seems to have grown and emerged in ca. 300 yr. Stabilization of the sand barrier occurred at some point during the 4th to 6th CE centuries, evidenced by the presence of a Roman salting fish factory (*cetaria*).

On the other hand, the general evolution of sand barriers and spits has been intensely studied in this area (e.g. Rodríguez-Vidal, 1987; Zazo et al., 1994, 2008; Goy et al., 2003). These studies have concluded that the growth of these sedimentary bodies has been produced by an alternation of progradation and no-growth or erosion periods conditioned by climatic variations that induced small sea-level changes (Goy et al., 2003; Zazo et al., 2008). Along the coast of Huelva four morpho-sedimentary episodes have been distinguished, punctuated by short periods of erosion (c.f. Zazo et al., 1994; Rodríguez-Ramírez et al., 1996). So, the  $^{14}\text{C}$  timing (H) for littoral progradation are  $H_1$  (6900 to 4500 cal. yr BP),  $H_2$  (4200 to 2600 cal. yr BP),  $H_3$  (2300 to 1100 cal. yr BP) and  $H_4$  (1000 cal. yr BP-Present), separated by erosion phases (4500 to 4200 cal. yr BP; 2600 to 2300 cal. yr BP; 1100 to 1000 cal. yr BP). These discontinuous progradation periods have been correlated with an increased aridity during Bond events (Zazo et al., 2008). Discrete sets of beach crests and swales on the surface of each unit are separated by erosional surfaces and/or particularly large swales called gaps (Zazo et al., 1994; Dabrio et al., 2000). They represent the sub-aerial record of the mid-late Holocene coastal wave action and the dominant southeastward drift current. These prograding morpho-sedimentary units occur as estuarine barriers on the Atlantic side of the Iberian coast and as barrier islands along the Mediterranean side. They are the emergent part of the Holocene highstand, which in the Atlantic-Mediterranean linkage area began ca. 6500 yr BP (Zazo et al., 1994; Dabrio et al., 2000).

The Saltés Island sandy formations have been considered part of the different Southern Iberian coastal progradation periods mentioned before (Lario, 1996; Dabrio et al., 2000). El Almendral and El Acebuchal (Fig. 1), located on the inner area of the Huelva Estuary, were formed during early stage  $H_2$ , whereas La Cascajera was formed later, most probably during two different phases (late  $H_2$  for its northern sector and  $H_3$  for its southern one). During the most recent progradation stage  $H_4$ , Cabezo Alto, the sand bar closest to the estuary's mouth, was formed, although it has suffered anthropogenic modifications during the last decades.

## 2.2. Coastal dynamics

The present-day climate of the Gulf of Cádiz can be defined as Mediterranean with Atlantic influence. The mean annual rainfall is around 600 mm, with an uneven distribution along the year (two maxima in late autumn and spring and a very dry summer). The mean annual temperature is 18 °C (with summer maximum around 40 °C). The prevailing winds come from the SW, while those coming from the SE and E are less common, but also important since they are associated with storm events, mostly during the winter season (Borrego, 1992). According to the statistic analysis of the recent storm record, these

high-energy periods are mainly concentrated in two months (December and January). Each storm period includes one to four storm families (1–7 days), being separated by 2–40 quieter days. An analysis of the individual storm features indicates a direct relation between the direction and speed of the prevailing winds and the causes of these events. In all cases, these winds come from the third quadrant. The maximum wave heights reach 5–8 m (Ruiz et al., 2005a).

This climatic setting determines the hydrodynamic characteristics of the south Atlantic Iberian littoral, mainly the fluvial regime, the wave actions and the southeastern drift currents. The Guadiana and Guadalquivir rivers (Fig. 1) are the main sediment source in this Atlantic coastal region, with a mean discharge of 144 and 185 m<sup>3</sup>/s, respectively (Vanney, 1970). The freshwater discharge of the Tinto and Odiel Rivers is subject to seasonal changes. The highest runoff occurs from December to February in both streams (an average of 100 hm<sup>3</sup>/month), and the lowest runoff occurs during the summer months (~1 hm<sup>3</sup>/month) (Borrego, 1992). These rivers are very polluted owing to historical mining activities, with very high concentrations of heavy metals, such as Cu, Pb or Zn (Ruiz, 2001). In addition, sediments derived from fluvial inputs are characterized by high percentages of quartz (50–80%), with feldspar and phyllosilicates as main accessories. Clay minerals are dominated by illite, with minor percentages of chlorite and kaolinite (Requena et al., 1991).

The prevailing wave direction is directly related to the wind regime, which is from the SW. Waves have a significant height of < 0.5 m over 75% of the year (MOPU, 1991; Borrego, 1992). This wave regime determines that the prevailing littoral drift is from W to E, with a mean sediment load estimated between 180,000 and 300,000 m<sup>3</sup> (CEEPYC, 1990; Cuena, 1991).

The tidal regime in this region is mesotidal (mean range 2.15 m, varying from 0.70 m during extreme equinox neap tide to 3.85 m during extreme equinox spring tide) and semidiurnal, with a low diurnal inequality (Borrego et al., 1993). The magnitude of the associated tidal currents is higher in the estuarine channels than on the open coast, and it also differs from flood to ebb conditions, ranging from 0.09 to 0.94 m s<sup>-1</sup> (Morales et al., 2004).

## 3. Materials and methods

Several outcrops located on the northwestern edge of La Cascajera were investigated in detail (Figs. 1 and 2), mainly from the sedimentological and palaeontological point of view, in addition to a superficial archaeological prospection of the surrounding. The current dynamics of a meandering tidal creek has eroded the northern edge of the sand barrier, exposing up to 3 m of littoral sub-aerial sediments during the mid-low tides. Three sectors within this edge were studied, namely West (WM), Middle (MM) and East Meander (EM), where six stratigraphic profiles were analyzed in detail after manually cleaning the outcrops and digging further below surface to a depth of 0.5 m below mean sea level. On these profiles, 72 samples were collected (Fig. 2) for textural, mineralogical, palaeontological, chronological ( $^{14}\text{C}$ -AMS dating) and archaeological analysis, as described as follows.

### 3.1. Textural, mineralogical and palaeontological analysis

The facies were characterized on the basis of the occurrence of sedimentary structures, bedding, bioturbation, etc., both in the field and by means of granulometric analysis, mineralogical composition and organic content of the obtained sediment samples (Table 1). For these analyses, sixty-six sediment samples were collected systematically of the different sedimentary units identified (Fig. 2). For the collection, a hand shovel was used to obtain approximately 1 kg of sediment, which was stored in resealable sample bag. The grain size distribution was determined by dry sieving of the coarse fraction (> 63 µm). Fine grained is referred to muddy sediments smaller than 63 µm (silt + clay).

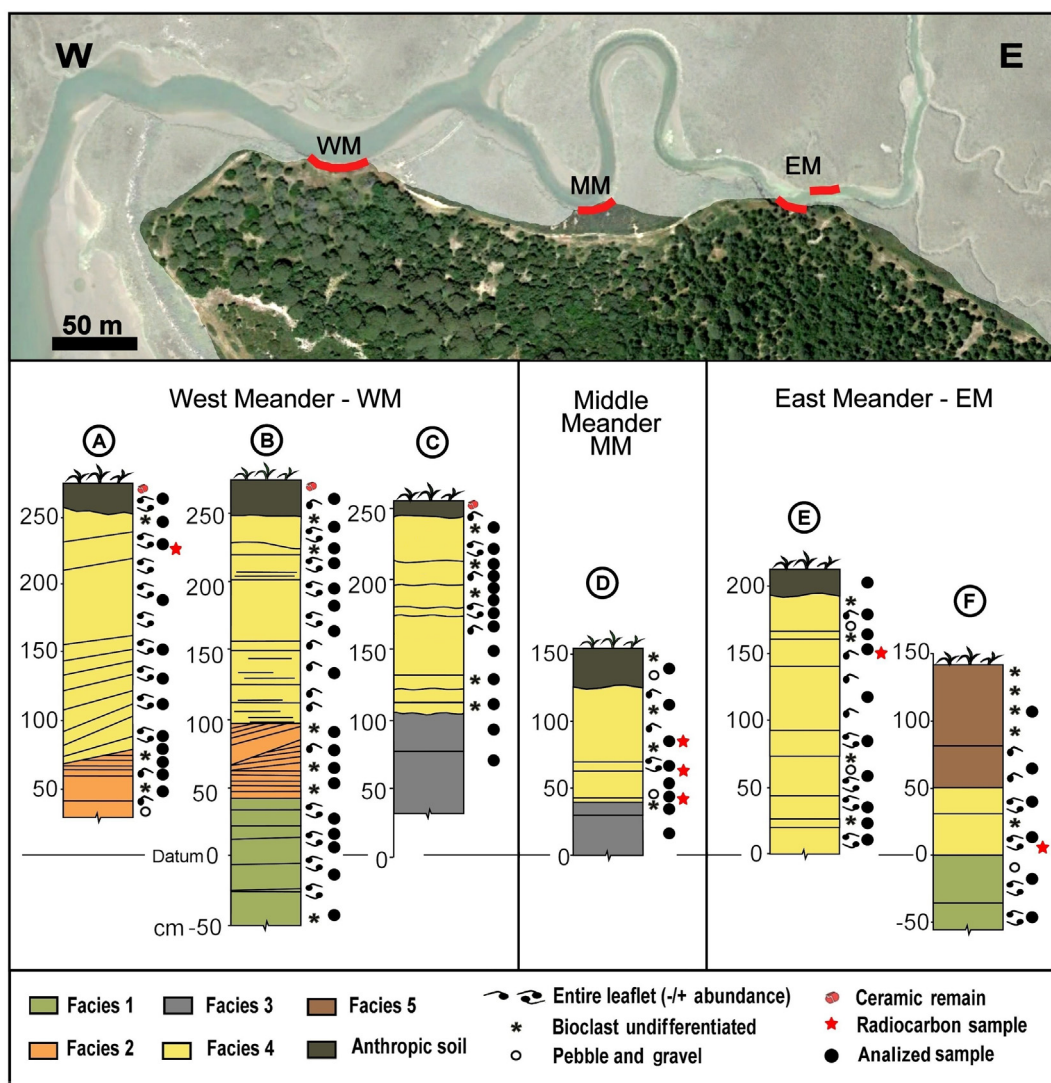


Fig. 2. Stratigraphic sections and sedimentary facies investigated along the NW shore of La Cascajera barrier on Saltés Island (see reference point in Fig. 1). (Image above by Google Earth.)

Mineralogical identification was performed on five sediment samples where the proportion of fines was higher. The analysis by X-ray diffraction (XRD) was done with a D8 Advance A25 Bruker diffractometer. Sediment samples were initially grinded and finely sieved ( $< 50 \mu\text{m}$ ). The software used was X Powder, in conjunction with the ICDD database (International Centre for Diffraction Data). XRD studies were performed both on bulk samples and mounted grain slides (using the  $< 20 \mu\text{m}$  fraction). The latter were used to potentially differentiate multiple types of sediments and their provenance (marine vs terrestrial). The mounted slides were air-dried, solvated with Ethylene Glycol, treated with Dimethyl Sulfoxide and heated at  $550^\circ\text{C}$ . When required, organic matter was initially eliminated using  $\text{H}_2\text{O}_2$ . The semi-quantitative estimation of the mineral content was carried out using the intensity factors (Gulbrandsen, 1960; Schultz, 1964; Barahona, 1974).

Macrofossils were separated after wet sieving (1 mm mesh). Foraminiferal assemblages ( $< 63 \mu\text{m}$ ) were obtained after wet sieving (adding Na-hexametaphosphate as a dispersing agent) a portion (50 g) of each sediment sample. This residual fraction was studied under a stereoscopic microscope in order to identify the presence of each foraminiferal assemblage. Taxonomical determination and taphonomic description was obtained on bivalves, gastropods and foraminifera, and density and diversity of the last group (Table 2 and Fig. 3). Relative abundance of other species such as scaphopods, barnacles, and

echinoderms was also obtained.

### 3.2. Radiocarbon analysis

Accurate dating is essential for the construction of reliable palaeoenvironmental and palaeoclimatic models based in multi-proxy analysis of sedimentary records. Radiocarbon ( $^{14}\text{C}$ ) dating is one of the most common methods used to build up chronological frameworks for the last 50,000 years. Six samples of marine shell *Glycymeris* sp. were collected for  $^{14}\text{C}$  dating (Fig. 2 and Table 3), directly from La Cascajera outcrops at various levels. Pristine shells, i.e. with no evidence of weathering, wear or breakage, were collected from the bio-clastic beds. The outermost layer of each individual shell ( $\sim 30\%$  by weight) was discarded by controlled acid etching (0.5 M HCl at  $25^\circ\text{C}$ ). The  $^{14}\text{C}$  content was measured by AMS at the Spanish National Centre for Accelerators (CNA). Conventional  $^{14}\text{C}$  dates were calculated in accordance with the definitions recommended by Stuiver and Polach (1977).

As it is known, the ocean reservoir is deficient in radiocarbon compared to the atmosphere, consequently, an offset in the  $^{14}\text{C}$  age (reservoir age) exists between coeval samples containing marine carbon versus those containing terrestrial carbon. So, a record of past reservoir ages is preserved in marine shells. The quantification of the marine radiocarbon reservoir effect ( $\Delta\text{R}$ ), defined as the difference between the



**Table 1**

Stratigraphic, sedimentological and mineralogical characteristics of the different facies and sub-facies differentiated in the study area.

Facies		Stratigraphy and sedimentology				Mineralogy								
		Granulometry (%)			Sorting	Sedimentary structures	Bulk mineralogy (%)			Fine fraction (< 20 µm) (%)				
		Gravel	Sand	Silt + clay			Quartz	Phyllosilicates	Feldspars	Illite	Kaolinite	Smectite	Chlorite	
1	Sandy tidal flat	1–30	60–80	< 2	Moderate	Massive	56–65	16–29	15–19	56–71	17–22	< 5–13	5–6	
2	Chenier	30–80	30–100	< 2	High	Planar stratification Cross-stratification Inverse gradation	No data			Very scarce fraction				
3	Tidal flat	30–40	< 2	80–90	Moderate to high	Massive	56–61	23–24	15–21	56–62	21–22	11–12	< 5–6	
4	Washover fans/ tempestite events	4.A: <i>Glycymeris violacescens</i> beds	> 90	< 10	< 1	High	Imbrication Parallel bedding	Mainly bioclasts						
		4.B: Bioclastic sands and gravels	20–65	20–75	< 3	Low to moderate	Erosive basal contact N-NW dipping	60	23	17	73	19	< 5	< 5
		4.C: Medium sands and gravels	30–65	20–80	< 5	Low to moderate	Normal gradation Parallel lamination							
5	Modern salt marsh	< 3	90	≤ 10	High	Massive	No data							

reservoir age of the mixed layer of the regional ocean, and the reservoir age of the mixed layer of the average world ocean in 1950 CE (Stuiver et al., 1986) is of crucial importance to the correct calibration of  $^{14}\text{C}$  ages of marine provenance. The  $\Delta R$  along the Andalusian Atlantic coast has been calculated at  $-108 \pm 31$   $^{14}\text{C}$  yr for the last 3000 years (Martins and Soares, 2013), which is in accordance with the oceanographic conditions present in the area. This value was taken into account when using MARINE13 calibration curve (Reimer et al., 2013) for

the conversion of conventional radiocarbon ages to calendar dates. This procedure was also applied to additional samples obtained by other authors in the Tinto-Odiel estuary (Goy et al., 1996; Dabrio et al., 2000) in order to draw a palaeoenvironmental evolution of this area (Table 4 and Fig. 8).

Results of La Cascajera are presented as calibrated ages for  $2\sigma$  intervals using a Bayesian model (see Results section and Fig. 7). Bayesian statistics details, a common practice for  $^{14}\text{C}$  dates modelling, are

**Table 2**

Palaeontological features of the different facies and sub-facies differentiated in the study area.

Facies		Palaeontology				
		Macrofauna			Microfauna	Taphonomy
		Bivalves	Gastropods	Others	Foraminifera (p: planktonic)	
1	Sandy tidal flat	<i>Glycymeris violacescens</i> <i>Chamelea gallina</i> <i>Dosinia lupinus</i> <i>Crassostrea gigas</i>	<i>Bittium reticulatum</i> <i>Mesalia varia</i> <i>Nassarius incrassatus</i>	Scaphopods ( <i>Dentalium</i> spp.)	<i>Ammonia beccarii</i> <i>Ammonia tepida</i> <i>Elphidium crispum</i> <i>Haynesina germanica</i>	Well preservation
2	Chenier	<i>Glycymeris violacescens</i> <i>Chamelea gallina</i> <i>Ostrea edulis</i>	<i>Calyptrea chinensis</i> <i>Nassarius incrassatus</i>	Scaphopods ( <i>Dentalium</i> spp.) Spines of echinoderms	<i>Ammonia beccarii</i> <i>Elphidium crispum</i> <i>Neoconorbina orbicularis</i> <i>Globigerinoides ruber</i> (p) <i>Orbulina universa</i> (p) <i>Ammonia beccarii</i> <i>Ammonia tepida</i> <i>Elphidium crispum</i> <i>Haynesina germanica</i>	Large number of small borings ( <i>Entobia</i> , <i>Caulostrepis</i> ) in mollusc shells
3	Tidal flat	Scarce shells of <i>Chamelea gallina</i> and <i>Cerastoderma edule</i>	Few specimens of <i>Bittium reticulatum</i> and <i>Mesalia varia</i>	No	<i>Ammonia beccarii</i> <i>Ammonia tepida</i> <i>Elphidium crispum</i> <i>Haynesina germanica</i>	Well preservation
4	Washover fans/ tempestite events	4.A: <i>Glycymeris violacescens</i> beds	<i>Glycymeris violacescens</i> (> 90%)	No	No	Borings, breakage of the umbo and surface abrasion
		4.B: Bioclastic sands and gravels	<i>Glycymeris violacescens</i> <i>Chamelea gallina</i> <i>Dosinia lupinus</i> <i>Crassostrea gigas</i> <i>Mimachlamys varia</i>	<i>Bittium reticulatum</i> <i>Mesalia varia</i> <i>Nassarius incrassatus</i>	Spines of echinoderms	<i>Ammonia beccarii</i> <i>Nonion commune</i> <i>Heterolepa bellincionii</i> <i>Triloculina trigonula</i>
		4.C: Medium sands and gravels	Similar to subfacies 4.B, with a scarcer bioclastic debris			
5	Modern salt marsh	<i>Glycymeris violacescens</i> <i>Chamelea gallina</i> <i>Ostrea edulis</i>	No	No	No	No

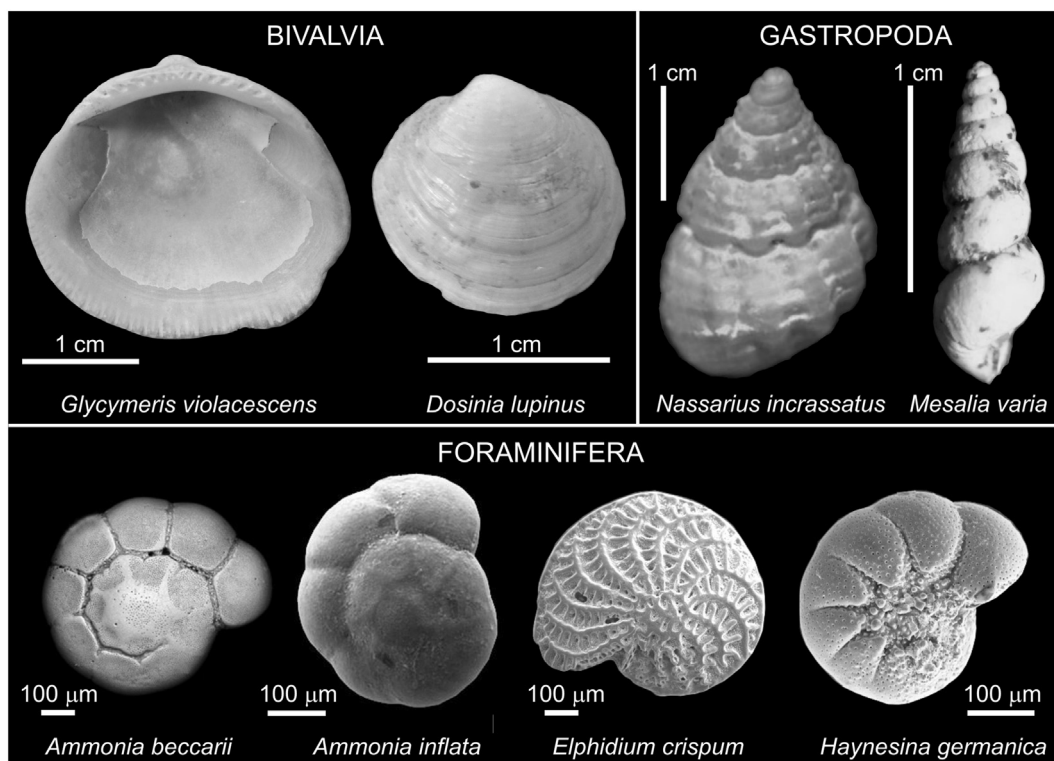


Fig. 3. Summary of the palaeontological record obtained at La Cascajera, with the most representative species of each group.

**Table 3**

Radiocarbon ages (non-calibrated and calibrated) and calendar dates for *Glycymeris* shell samples collected across the tempestite facies of La Cascajera outcrops.

Field code Field location	Lab. code	<sup>14</sup> C age yr BP	Calibrated date (2σ) <sup>a</sup> unmodelled	Calibrated date (2σ) <sup>a</sup> modelled
Start boundary				154 BCE–96 CE
<i>East meander</i>				
HUCA-1301	CNA-2817	2263 ± 31	167 BCE–71 CE	104 BCE–99 CE
HUCA-1401	CNA-2820	2210 ± 32	112 BCE–135 CE	54 BCE–127 CE
<i>Middle meander</i>				
HUCA-1405	CNA-2823	2172 ± 32	65 BCE–182 CE	65 BCE–114 CE
HUCA-1406	CNA-2824	2150 ± 33	33 BCE–214 CE	39 BCE–132 CE
HUCA-1407	CNA-2825	2170 ± 32	61 BCE–186 CE	31 BCE–151 CE
<i>West meander</i>				
HUCA-1303	CNA-2819	2189 ± 31	87 BCE–153 CE	56 BCE–131 CE
End boundary				29 BCE–204 CE

<sup>a</sup> Calibrations done using the MARINE13 calibration curve (Reimer et al., 2013), OxCal v4.2.4 (Bronk Ramsey, 2001, 2009), and a  $\Delta R = -108 \pm 31$  yr <sup>14</sup>C (Martins and Soares, 2013).

described in several papers (c.f. Buck et al., 1991, 1992; Bronk Ramsey and Allen, 1995), as well as the mathematic models used by OxCal, which not only is used for the calibration of conventional <sup>14</sup>C ages, but also used for statistical modelling (Bronk Ramsey, 2001, 2008, 2009). It allows for the reduction of the uncertainty associated with the calibration process, through the incorporation of information related to various constraints, such as the stratigraphic sequence from which the dated samples were collected. Due to the incorporation of this information in the model, a subsequent uncertainty distribution is obtained for each age and, consequently, new limits for the time interval

of the calibrated date (Bronk Ramsey, 2001, 2008, 2009). For these <sup>14</sup>C ages presented herein, the Bayesian model was set up with OxCal v.4.2.4 (Bronk Ramsey, 2001, 2009, 2012) using MARINE13 calibration curve (Reimer et al., 2013).

### 3.3. Archaeological remains

This investigation and palaeogeographic reconstruction of the Huelva Estuary has taken into account all previously published studies related to coastal prehistoric and historic archaeological sites found in the region (Fig. 4; for recent reviews see Campos et al., 1999, 2002, 2014). This approach allows for a more multi-disciplinary and general perspective of the human settlement patterns in relation with the morphodynamic coastal evolution during the mid-late Holocene.

The recently discovered Roman archaeological site (Fig. 4) of La Cascajera (Rodríguez-Vidal et al., 2014) was hidden by an organic-rich soil and a dense vegetation cover, difficulting all prospection. No systematic excavation has yet been performed at this site, but initial surface prospection reconnaissance points at the northwestern edge of the sand barrier as the most archaeologically-rich. The typological and chronological identification of the abundant ceramic materials so far discovered on the soil surface and deeper along some outcrops was carried out. Sherds were systematically collected, cleaned and sorted, allowing for an initial archaeological analysis of La Cascajera.

## 4. Results

### 4.1. Facies and palaeoenvironmental interpretation

The study of the deposits outcropping at La Cascajera barrier, central sector of Saltés Island, has allowed distinguishing five sedimentary facies that constitute a typical association of an estuarine marine environment (Fig. 2 and Table 1), showing different degrees of marine influence and little or no fluvial input.

**Table 4**

Radiocarbon ages (non-calibrated and calibrated) and calendar dates obtained from previous works in the Huelva Estuary (location is detailed in Fig. 8).

Sample code	Field location	Laboratory code	Fig. 8	<sup>14</sup> C age yr BP	Error	Calibrated date (2σ) unmodelled		References
						BP	BCE–CE	
PU95-2	Punta Umbria spit	GX-20908	1	3555	75	3795–3380	1850 BCE–1430 BCE	Goy et al. (1996)
PU95-1	Punta Umbria spit	GX-20907	2	3315	70	3470–3070	1520 BCE–1125 BCE	Goy et al. (1996)
HU94-9	Punta Arenilla spit	IRPA-1156	3	3220	95	3410–2900	1460 BCE–960 BCE	Dabrio et al. (2000)
HU94-8	Punta Arenilla spit	IRPA-1164	4	2950	95	3140–2640	1190 BCE–695 BCE	Dabrio et al. (2000)
HU94-3	La Cascajera (Saltés Island)	IRPA-1157	5	2705	90	2750–2320	800 BCE–370 BCE	Dabrio et al. (2000)
HU94-4	La Cascajera (Saltés Island)	IRPA-1158	6	2675	90	2730–2305	780 BCE–360 BCE	Dabrio et al. (2000)
HU94-2	El Acebuchal (Saltés Island)	UtC-4185	7	1900	105	1820–1325	130 CE–625 CE	Dabrio et al. (2000)
PU95-3	Punta Umbria spit	GX-20909	8	1900	70	1770–1380	180 CE–570 CE	Goy et al. (1996)

4.1.1. General facies

4.1.1.1. Facies 1: sandy tidal flat ( $\pm 0.5\text{ m}$  about mean sea level - a.m.s.l.). The basal deposit of La Cascajera consists of fine to medium sand and gravel with abundant mollusc shells, located in the intertidal zone of this area. These medium to coarse sediments are interspersed

with organic-rich silts and a 12 cm thick layer of red clay in the upper part. The bulk mineralogy is dominated by quartz (Table 1: 56–65%), while the mineralogical assemblage (< 20  $\mu\text{m}$  fraction) is mainly composed by illite (56–71%).

Marine and brackish bivalves such as *Glycymeris violacescens* (Fig. 3;

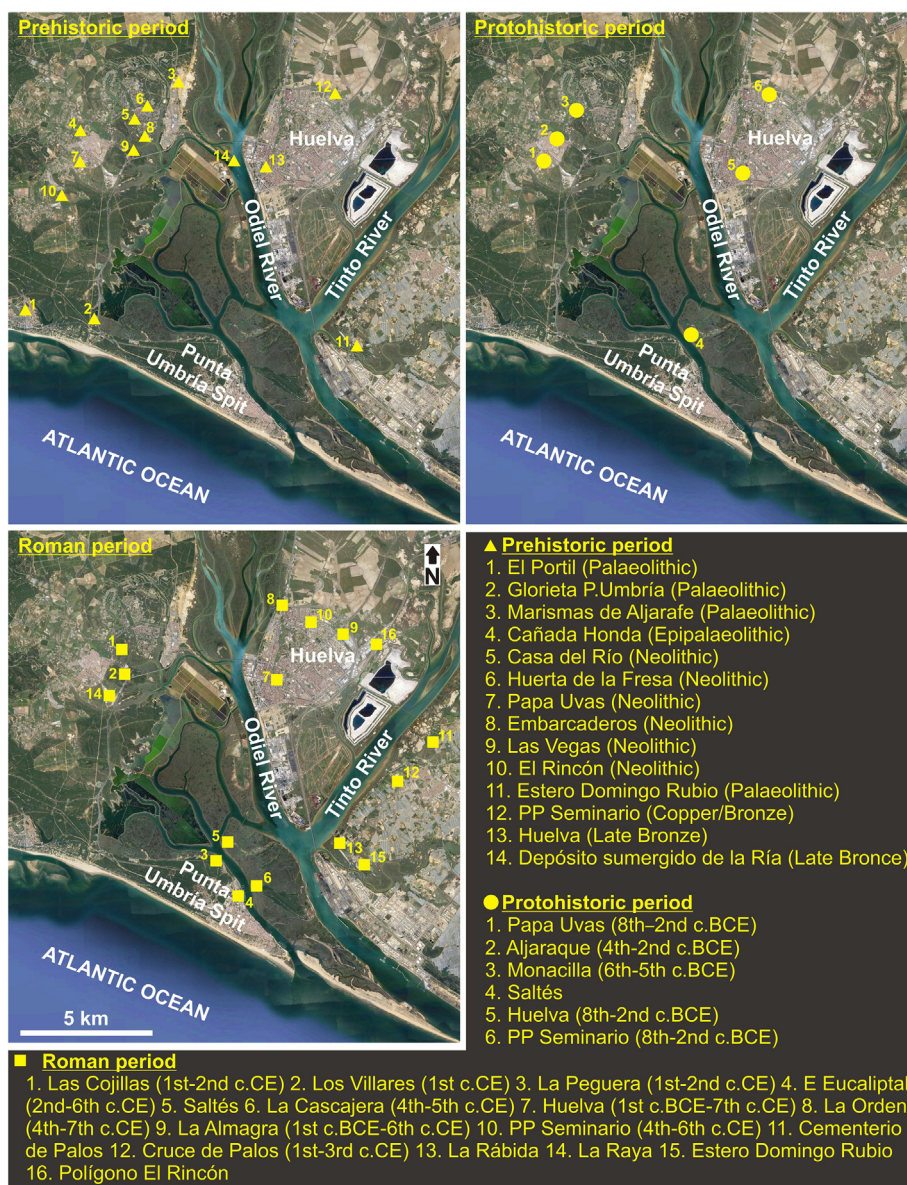


Fig. 4. Location of archaeological sites of different cultural periods around the Huelva Estuary. (Map by Google Earth.)



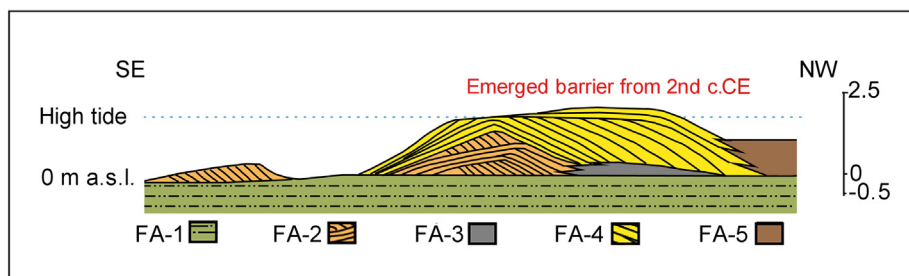


Fig. 5. Interpretative cross-section of La Cascajera barrier and distribution of its sedimentary facies.

synonymous of *Glycymeris nummaria*), together with marine gastropods (*Bittium reticulatum*), scaphopods (*Dentalium* sp.) and others (Table 2) are common in this facies. Benthic marine and brackish foraminifera (Fig. 3: *Ammonia beccarii*, *Ammonia tepida* and *Elphidium crispum*) have been also picked in these sediments. All these specimens are well preserved and show no evidence of marked abrasion or bioerosion, which indicates little or no transport from its source.

The red clay level denotes the oxidation of organic matter due to intermittent sub-aerial exposure. In addition, the biological assemblages have been previously described in shallow areas (< 25 m) of the southwestern Spanish shelf (c.f. González-Regalado et al., 2001; Gómez Álvarez, 2013). Therefore, this facies represent a sandy shoal or protected sandy tidal flats (Fig. 5), located close to the river mouth within the estuary that was periodically submerged by tides.

**4.1.1.2. Facies 2: chenier (0.5–1 m a.m.s.l.).** Facies 2 appears overlying facies 1, only from the middle to high intertidal zone of WM (see profiles A and B, Fig. 2). It consists of decimetre-thick layers bio-clastic gravel and coarse sand with very scarce silty-clayey matrix (Table 1). These facies remain submerged during high tides or storm periods.

Marine macro-fauna is abundant in this facies (Table 2), with numerous rounded fragments of molluscs, including bivalves (*G. violascens*, *C. gallina*), some scarce gastropods and scaphopods, as well as spines of echinoderms. Reworked marine benthic (mainly *A. beccarii* and *E. crispum*) and planktonic (mainly *Orbulina universa*) foraminifera are also abundant. A high percentage of molluscs show a large number of small borings (i.e. bio-erosive activity).

At present, the described species inhabit modern littoral environments in the Gulf of Cádiz (c.f. Pérez Quintero, 1989; Junta de Andalucía, 1993). The roundness of the mollusc fragments, some of which also present borings (e.g. *Entobia*, *Caulostrepsis*), indicates intense transport processes. Based on the proximity of occurrence of similar species at present, it is possible to assume a local provenance for the identified species in Facies 2. This facies is interpreted as a shell barrier or chenier with a steep lee side (Fig. 5), allowing for rapid inland migration (c.f. Augustinus, 1989; Otvos, 2000). This interpretation agrees with that deduced by Morales et al. (2014) on the basis of other sections of Saltés Island and the evolution of the southernmost part of this Biosphere Reserve during the last decades.

**4.1.1.3. Facies 3: tidal flat (0.5–1 m a.m.s.l.).** These sediments represent a lateral change of facies 2, with a similar vertical distribution in relation to the mean sea level. They are constituted by massive, blueish-grey sandy silt (Table 1), intensively burrowed by annelids with scattered mollusc shells. Facies 3 is mineralogically similar to facies 1, predominantly composed of quartz (56–61%), with illite (56–62%) as main component of the finer fraction (< 20 µm).

This facies presents low abundance of bivalves, such as the marine species *C. gallina* or the brackish species (*Cerastoderma edule*), together with scarce marine gastropods (Table 2). The microfauna is represented by brackish and marine specimens of foraminifera (*A. beccarii*, *A. tepida*, *H. germanica*).

The species present in facies 3 are commonly found in modern

channelled estuaries and coastal lagoons restricted by sand bars, at depths varying from 0 to –15 m a.s.l. (González-Regalado et al., 2001; Gofas et al., 2011). Facies 3 is interpreted to represent a silty tidal flat on the lee side of a chenier (Fig. 5).

**4.1.1.4. Facies 4: washover fans/tempestite events (1–2.5 m a.m.s.l.).** Facies 4 is a bioclastic-rich sand (Table 1) located in the supra-tidal zone (only submerged during equinox tides or extreme storm periods), outcropping over the entire studied northern edge of La Cascajera (Fig. 2). Quartz (60%) and phyllosilicates (23%) are the main mineralogical constituents, whereas the finer fraction dominated by illite (73%). Facies 4 also records a lateral change towards the western edge of WM (profile A, Fig. 2), where 5–30 cm thick layers show erosive surfaces that are overlaid by quartz pebbles and mollusc valves of *Glycymeris* and *Chamelea*.

Mollusc shells are present throughout the unit mainly as scattered valves and abundant fragments of bivalves and gastropods (Table 2). The bivalve shells show evidence of transport and impact (loss of the umboes, abrasion of ornamentation, valves break and fragmentation), indicating high-energy environment. In addition, some incrusting organisms (annelids, crustacean barnacles) are frequent on these shell surfaces.

If present, the associated microfauna is represented by a marine benthic foraminifera assemblage (*A. beccarii*, *N. commune*, *H. bellionii*, *T. trigonula*).

The foraminiferal assemblage associated to this facies are well represented in modern marine coastal environments (from depths of –20 to –30 m a.s.l.) along the Iberian Peninsula, subject to the action of strong-tidal currents and waves (c.f. González-Regalado et al., 2000), such as the case of the Huelva Estuary. Facies 4 is therefore interpreted as washover fans that overran the barrier island during storm events. A series of tempestite events are clearly visible in the northwestern edge of La Cascajera that formed the accumulation of successive shell-rich storm layers by re-working and subsequent overwash of previous sand barrier deposits (Figs. 5 and 6).

Three major sub-facies were identified, and due to the importance of facies 4, they are detailed in a section below.

**4.1.1.5. Facies 5: modern salt marsh (0.5–1.4 m a.m.s.l.).** Facies 5 is constituted by organic-rich sediments corresponding to the modern estuary marshland, located generally in the supratidal zone. It only outcrops at the top of EM (as seen in profile F, Fig. 2). This salt marsh has an average thickness of 1 m. The lowermost 30 cm of this unit is composed of well-sorted fine to medium sand (sand: 90%) and few fragments of molluscs, whereas the uppermost 60 cm are composed of silty sand (Table 1), showing an erosive basal contact and massive bedding. It is characterized by the presence of halophyte vegetation of the *Spartina*, *Salicornia* and *Sarcocornia* genera. This facies is intensely bio-turbated by crustaceans and annelids. The macro-fauna is scarce in the lower part (mainly *G. violascens*) and absent in the upper part. No evidence of micro-fauna has been observed.

This unit was deposited in a brackish marsh environment frequently flooded by tides (Fig. 5), hence the regular infilling and subsequent



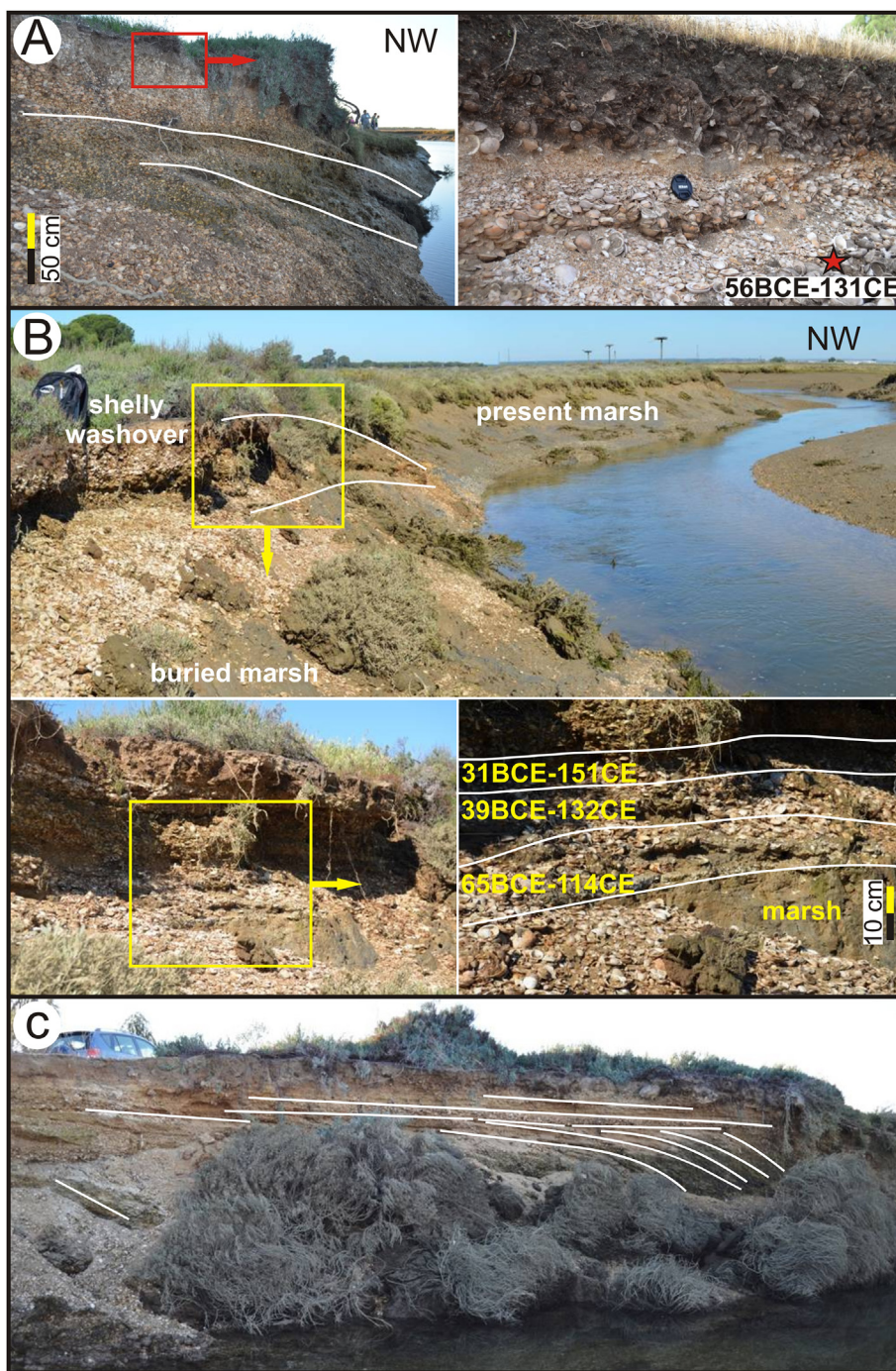


**Fig. 6.** Photographs of outcrops detailing the ages of the different tempestite units along the NW edge of La Cascajera barrier. A: WM, with sub-facies 4.A and location of  $^{14}\text{C}$  sample. B: MM, sub-facies 4.C and its corresponding age sequence. C: EM, detail of the tempestites' sedimentary structures.

emersion of the inner part of the estuary (EM), allowing the colonization of diverse terrestrial plant and animal species. These sediments have high organic matter content due to the degradation and accumulation of plant debris.

#### 4.1.2. La Cascajera tempestite facies

The general description of this washover event sequence was given in the previous section (Facies 4). A more detailed characterization of this thick and important unit that forms most of La Cascajera barrier is given as follows (see Fig. 6). Facies 4 is mainly composed of bio-clastic sandy sediments resulting from re-working of quasi-contemporary previously deposited nearby cheniers and tidal flats.

**4.1.2.1. Sub-facies 4.A (0.7–2.5 m a.m.s.l.).** It is characterized by the accumulation of successive layers of disarticulated and unbroken *Glycymeris violascens* shells (> 90% dry weight) with very scarce clay matrix (Fig. 6A). Borings, breakage of the umbo and slight to moderate surface abrasion are also visible. No evidence of microfauna was observed. These shell layers have variable thickness (1–15 cm) and are alternated with thin secondary clay layers. They show an erosional surface that dips SE-NW, commonly showing imbrications of shells and/or parallel bedding. This sub-facies overlays the chenier sediments (Facies 2) but it disappears towards the East by means of a lateral change of facies towards sub-facies 4.B.

The moderate abrasion, breakage and presence of borings on most

of the bivalves in this unit together with the dipping of the layers indicates short transport processes, mostly from SE to NW, by the action of high-energy marine episodes. This direction is partially conditioned by the growing of the Punta Umbría spit and the presence of an adjacent channel during this storm period (see Fig. 8).

These processes supplied materials readily available nearby (i.e. inter-tidal and sub-tidal zones) to this supra-tidal environment. Both the concentrations of bivalves and the thickness of the superimposed shell-rich layers correspond to the sum of several storm events leading to the vertical accretion of tempestite deposits. The absence of microfauna may be due to the absence of matrix by washing the fine fraction during these high-energy events. This absence has been observed in other high-energy deposits of southwestern Spain (Ruiz et al., 2005b).

**4.1.2.2. Sub-facies 4.B (1–2.5 m a.m.s.l.).** This sub-facies is composed of bio-clastic coarse-medium sand and gravel with minor fines (Table 1). This deposit overlays the sandy tidal flat (Facies 1) or the chenier (Facies 2), forming beds 20–50 cm-thick. It presents an erosive and warped basal contact, capped by shell-rich and bio-clastic fragments layers, with variable percentages of sandy matrix. This sub-unit shows a clear N-NW dipping with a steep foreset ( $> 30^\circ$ ) that defines progradational and lateral accretionary processes.

In this sub-facies, complete, broken and disarticulated shells as well as shell fragments and debris of numerous mollusc species are highly abundant (Table 2), as well as echinoderm spines. All species show signs of abrasion and bioerosion.

The species identified in sub-facies 4.B currently inhabit shallow littoral environments (depths from 0 to  $-50$  m a.s.l.) around the Gulf of Cádiz (c.f. Pérez Quintero, 1989; Junta de Andalucía, 1993). The sedimentological and taphonomic characteristics indicate exposure to high-energy events. During storm episodes, the detrital material and biological component overran the chenier bars by high-energy wave action. Hence, each sedimentary bed is a record of a washover fan that was produced during a storm event, that subsequently prograded inland, episodically, creating the accretion features of this tempestite facies (Fig. 6C). The thicker layers that outcrop on WM correspond to the proximal sector of the washover fans.

**4.1.2.3. Sub-facies 4.C (0–2.2 m a.m.s.l.).** It consists of bio-clastic medium-fine sand and gravel. These 30–40 cm-thick beds are normally graded, and show diffuse parallel lamination, commonly defined by changes in grain size (Fig. 6B). These deposits correlate laterally with sub-facies 4.C and are widely represented in WM (Profile C), MM (Profile D) and EM (Profiles E and F) (Fig. 2). In this sub-facies, the bio-clastic debris is scarcer than in sub-facies 4.B. The microfauna is abundant with marine benthic foraminifera assemblage (Table 2) that show clear evidence of transport and re-working due to the consistent loss of the last chambers in miliolids and occurrence of fragments of planktonic species.

The most abundant microfaunal assemblage present in this sub-facies is the one that characterizes modern open shallow areas and estuary mouths in the southwestern Spanish shelf ( $< 20$  m depth), which is constantly under the action of strong tidal currents and waves (González-Regalado et al., 2001). During storm episodes the finest material, together with some bio-clastic debris, were eroded from the coastal and shallow marine environments, transported by the waves to the most protected areas of the back-barrier, and deposited in the distal areas of the washover fans (MM and EM).

## 4.2. Radiocarbon chronology

$^{14}\text{C}$  ages of marine shells and corresponding calibrated dates using the MARINE13 calibration curve (Reimer et al., 2013) are listed in Tables 3 and 4 and the Bayesian model graph is Fig. 7. There are three groups of dates, two of them constituting sequences of dates (EM and MM, Fig. 6B) while for WM there is only one date (Fig. 6A). On the

other hand, the chronological relationship between the three sectors is unknown because their morphology is hidden below recent dunes and vegetation.

The modelled calibrated  $^{14}\text{C}$  dates (Fig. 7) provide a time range between the second half of first century BCE and the first half of the second century CE for the deposition of the marine shells in the different outcrops recorded at the western edge of La Cascajera sandy barrier. Nevertheless, radiocarbon data does not allow differentiating chronologically the deposition order on the three sampled sectors.

Considering all these ages, the definitive emersion of La Cascajera barrier was probably produced during the 2nd century CE and the studied tempestite sequence represents a maximum of 150 years of severe storms activity.

## 4.3. Human settlement

The regional knowledge related to archaeological sites, previously published over the last decades (Campos et al., 1999, 2015), and the associated environmental and land use significance has allowed us to better understand the relationship between human settlement patterns and the Holocene morpho-sedimentary landscape evolution of the Huelva Estuary.

The oldest archaeological sites are Upper Palaeolithic (Fig. 3). Although it is not possible to precise a specific ascription (i.e. Glorieta de Punta Umbría in García Rincón and Rodríguez-Vidal, 1990), they are located in old fluvial terraces of the Odiel river and the lithic remains are linked to hunter-gatherer populations, without evidence of marine fauna consumption. The original locations of these sites were on the slopes of fluvial valleys as, during the Last Glacial lowstand, sea-level reached its lowest position, hence the shoreline was located further offshore and the current estuaries were not yet formed.

During the last maximum transgression, ca. 6500 yr BP, some Neolithic human settlements (Fig. 2) were associated with the palaeo-shoreline of the Huelva Estuary, although most of them were located more distant of shoreline (just over 1 km) and related with tributary inlets (small flooded valleys). Papa Uvas site is one of these places, where both farming and marine resources (e.g. fish, cetacean, molluscs) were exploited, as evidenced by the oldest stages of this settlement (Martín de la Cruz, 1998).

Dating of archaeological remains in El Almendral barrier on Saltés Island (Fig. 1) and its underlying sediments (Bazzana and Bedia, 2005) display that during the Chalcolithic and the Bronze periods (4th–1st millennium BCE) this barrier had not yet emerged. The Huelva Estuary was a wide bay where the only important coastal settlement was *Onoba* (ancient settlement in Huelva promontory). The Huelva site (Late Bronze, triangle no.13 in Fig. 3; Gómez Toscano and Campos Carrasco, 2001) proves a close connection between human activities and the sea: feeding habits and foreign trade evidence have allowed defining this site as a harbour city of great importance in the Late Bronze age. During this period, intensive mining (Olías and Nieto, 2015) generated great sediment supply to the estuary, which in turn facilitated the development of extensive salt marshes and the increase in brackish fauna productivity.

During the Proto-historic period, 8th–2nd centuries BCE, some continuously-inhabited settlements, such as Papa Uvas (circle no.1 in Fig. 3), still existed even though the economy of the time was more focused in a few important old sites (e.g. *Onoba*) and new coastal settlements (e.g. Aljaraque and Saltés). It was the moment of colonization of the estuary in terms of exploitation of food resources and commercial activities (Bermejo et al., 2016).

During the Roman period (Fig. 3), from the beginning of the 2nd century BCE to 6th century CE, there was an increase in natural resources exploitation (Campos et al., 2015). Agriculture, cattle rising, mining, among others, had a profound impact on the natural landscape, which in turn favoured soil erosion and sediment surplus, dramatically reducing the permanently flooded areas around the estuary (this is the



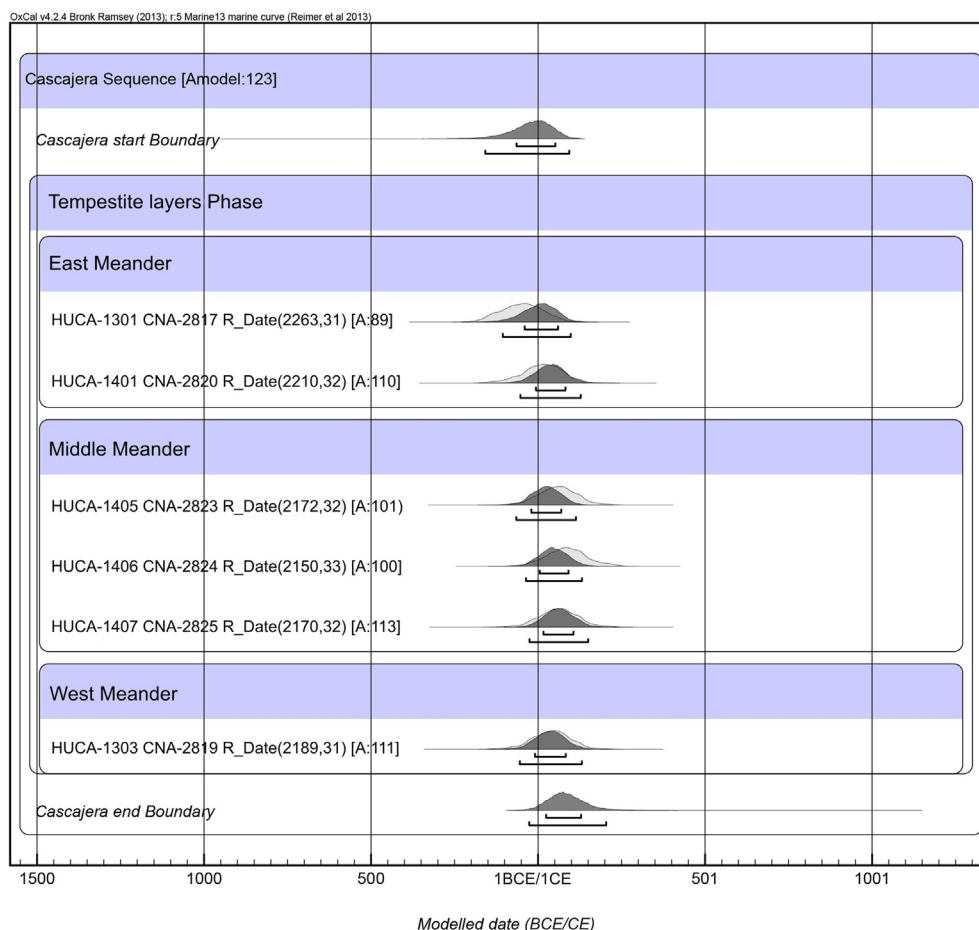


Fig. 7. Graphical representation of the calibrated radiocarbon age dataset (OxCal v.4.2.4) obtained for this investigation.

*Palus Erebea*, historical Roman name of the Estuary of Huelva).

The rapid growth of the Punta Umbría and Punta Arenilla littoral spits (see Fig. 1) and the development of estuarine sand barriers (such as La Cascajera) allowed the generation of new shorelines and a progressive estuarine offshore migration. The coastal Roman fish and salting factories (i.e. *cetariae*) either reused old settlements (such as *Onoba*) or were relocated closer to the shoreline. Examples of the latter are the Roman sites of La Peguera, El Eucaliptal and La Cascajera (see Fig. 3), which serve to define the ancient coastline.

## 5. Discussion

The interrelationship between the archaeological findings, the coastal geomorphology and the morpho-sedimentary evolution at the mouth of the Tinto and Odiel rivers allows us highlighting not just the Huelva Estuary evolution but also the possible patterns of human settlements since the beginning of the present highstand, i.e. since ca. 6500 yr BP. This evolution can be used as a man-environment interaction model to understand the complex evolution of other estuaries along the Atlantic Iberian coast.

### 5.1. La Cascajera barrier: morpho-sedimentary evolution

From the geological and chronological data it is possible to establish the recent development and evolution of La Cascajera barrier. First, the model proposed by Morales et al. (2014) seem to be partially confirmed for the sand formations of Saltés Island as they are interpreted as a chenier plains that served as an submerged obstacle for the storm waves, > 2000 years ago. On the studied outcrops in La Cascajera, no ages older than 100 yr BCE has been obtained which implies that the

development of this barrier should have initiated from that moment on, probably during the 2nd–1st centuries BCE. The *terminus ante quem* for the initial stage of the barrier development corresponds to the formation of a sandy tidal flat (Facies 1; Figs. 2 and 5). This flat covers sedimentary beds interpreted as small previous deltaic formations or sandy shoals in numerous cores (Borrego et al., 1999; Dabrio et al., 2000) and confirmed in present-day research (Rodríguez-Vidal et al., 2014).

The mineralogical analysis of the fine sediment fraction (< 20 µm) reflects the same mineral association in all the identified and described facies. However, it should be noted that there is a high illite content in facies 1, as opposed to the smectite and kaolinite content, reflecting a greater marine influence (Fernández Caliani et al., 1997). Such influence corresponds with the initial development of the tidal flat at the mouth of the estuary. Its construction started from an ebb tidal delta system (Morales et al., 2014), formed by the continuous accumulation of re-worked sediment of marine origin. These shoals reduced wave energy at the mouth of the estuary, facilitating continuous infill with finer sediments and only during spring tides waves were able to develop sandy bars that migrate inland.

Using this mechanism, the chenier was progressively built over the sandy tidal flat (Facies 2; Figs. 2 and 5) and it continuously migrated towards more internal and protected areas of the estuary as indicated by the well-developed chenier foresets. According to Morales et al. (2014), the chenier can be formed by a larger sand supply to the front of the tidal flat as a consequence of the eastern levee migration of the ebb tidal delta main channel. These authors explain that this is a cyclic mechanism during high tides, of primary marine influence, explaining why it mainly occurs presently at the Punta Umbría channel mouth that has no connection with the rivers.



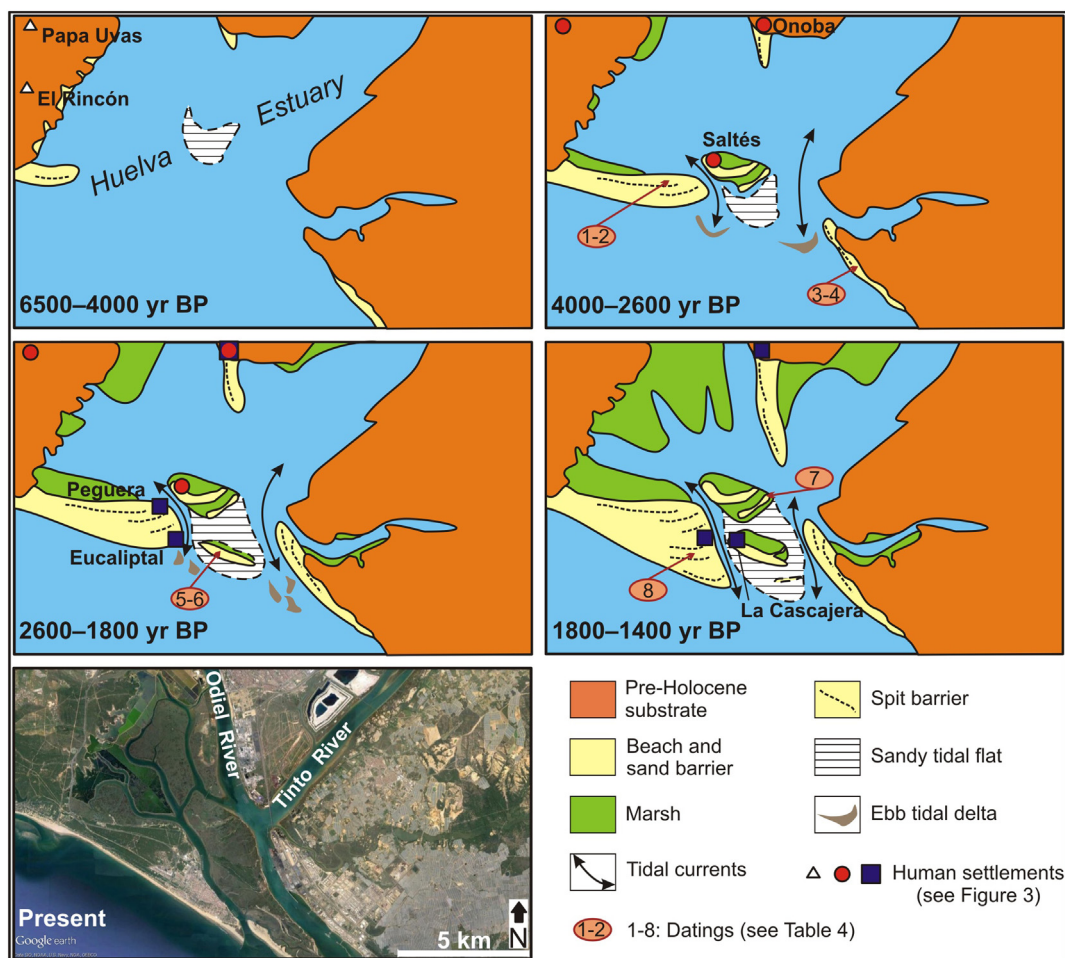


**Fig. 8.** Proposed interpretation model for the mid-late Holocene palaeogeographic evolution of the Huelva Estuary and timing for the post-6500 yr BP human settlement development: open triangles depict Pre-Historic period sites; blue squares represent Roman period settlements; and red circles Proto-historic period locations. (For interpretation of the references to colour in this figure legend, the reader is referred to the web version of this article.)

The chenier bar grew as it migrated towards the NE until it got an adequate size for its stabilization. This only occurs when the Mean Spring High Water Level height is surpassed. As a consequence of La Cascajera barrier growth and stabilization, a silty tidal flat developed in the intertidal zone protected by the chenier (Facies 3; Figs. 2 and 5). Due to its higher fluvial influence, product of its more up-estuary location, this facies shows a higher smectite and kaolinite content, as opposed to the more marine-influenced initial barrier phases.

Once the chenier stabilized, it became an obstacle for storm waves, the only effective natural process to affect its morphology. In a partially open estuary (Fig. 8), high-energy waves that overran the barrier and accumulated bio-clastic-rich sandy sediments and siliciclastic gravels atop the chenier and the adjacent saltmarsh in the form of washover fans (Facies 4; Figs. 2 and 5). These beds were formed by the successive amalgamation of reworked sediments that originally formed the coastal morphologies, such as the spits, foredunes or cheniers neighbouring La Cascajera (Sub-facies 4.B and 4.C). The taphocoenosis formed by the *Glycymeris* shells along La Cascajera is very similar to the one occurring along modern nearby beaches succeeding winter storms. The re-sedimentation of this reworked fauna originated Sub-facies 4.A. On the other hand, similar to what occurs in facies 1, the illite content increases while the smectite and kaolinite content decrease, reflecting yet again, a greater marine influence in accordance with the above explanation.

The thickening of facies 4 and its vertical overlapping indicate a very effective bed stacking mechanism over the chenier bar by means of progressive vertical aggradation and migration towards the N-NE from

the redistribution of sediments by high-energy waves.

Radiocarbon-AMS dating (Table 3 and Fig. 7) obtained from *Glycymeris* shells show that the upper facies of La Cascajera barrier was developed in a short period of time. Its appearance in a sub-tidal environment has to be established at the end of the second century BCE, while during the end of the first century BCE and along the first century CE the accumulation of tempestite beds increased the barrier's height above the tidal level (Fig. 5). The  $^{14}\text{C}$  dates model (Table 3 and Fig. 7) highlights that these high-energy deposits possibly record storms occurring during a period of approximately 100–150 years. This storm activity period agrees with one recorded in the Central and Northern Atlantic (Sorrel et al., 2012).

This sedimentary sequence, with multiple levels and coherent  $^{14}\text{C}$  ages (Fig. 6) in a time period of around 150 years, does not correspond to a typical tsunamis deposit, such as those already studied in this region (Ruiz et al., 2005b, 2008, 2013; Morales et al., 2008; Rodríguez-Vidal et al., 2011; Font et al., 2013).

The described above stage of growth allowed the definitively emergence of the barrier and the protection to continuous flooding, also favoured by the progradation off spits and beaches. Spits were attached to the eastern sector of these high-energy deposits (Fig. 1), due to the W-E direction of the coastal drift streams in this area (Cuena, 1991).

Despite this stabilization, it was not until the 4th century CE that the establishment of the Roman fishery industry (*cetariae*) occurred (Campos et al., 2014). There is still no record of any settlement in La Cascajera that precedes the latter. Furthermore, this moment agrees with definite spike in both fishing and food processing Roman

industries along the coasts of the Gibraltar Strait and the Gulf of Cádiz (Campos et al., 2015).

### 5.2. Huelva Estuary: morpho-sedimentary evolution, palaeogeography and human settlements

There is no direct evidence along the Atlantic Iberian coast of any littoral formation emerging at the maximum present Interglacial (6500 yr BP). At this time, the southwestern Spanish estuaries were flooded and the Tinto-Odiel estuary was a bay (Dabrio et al., 2000). The available data (e.g. Borrego et al., 1999; Dabrio et al., 2000) shows that between this maximum highstand and 4000 yr BP, the estuary started to infill with fluvio-marine bedload sediments. Concurrently, development of sandy-silt beaches occurred at both mouth margins. During this period, corresponding to part of the Neolithic and early Chalcolithic, human settlements were not directly associated with the marine environment and they located in the nearby hills (Figs. 4 and 8) as feed resources were mainly depended on the farming.

From 4000 to 2600 yr BP, the estuarine landscape started a dramatic change (Fig. 8). The increase in sedimentary supply generated by intense marine erosion of neighbouring rocky and sandy promontories, but also and more importantly, from fluvial input due to increased mining (Leblanc et al., 2000) and deforestation (Domínguez-Delmas et al., 2015), initiated the estuary's major infilling and re-shaping phase. These changes have also been recorded in other estuaries of the Southwestern Atlantic Iberian coast for this period (Schneider et al., 2016). The main changes occurred at the spits near the Odiel-Tinto mouth (Punta Umbría and Punta Arenilla in Rodríguez-Ramírez et al., 2000), along the interior attached beaches and in the sheltered marshes. The main settlement was the site city of *Onoba* (Huelva) that dominated a wide bay during the Chalcolithic and Bronze Age (Fig. 8). Evidence of an intrinsic relationship with the sea is clear in terms of marine navigation, trade and use of marine resources (Gómez Toscano and Campos Carrasco, 2001).

From about 2600 yr BP, the environmental conditions favoured the development of the first chenier-plain on the present Saltés Island (Fig. 8). The first formed sand barriers (El Almendral and El Acebuchal) should have developed following the same geological processes identified for La Cascajera and describe above, possibly emerging around 3000 yr BP (Dabrio et al., 2000). This time also coincides with storm periods in northern and central Europe (Holocene period III of Sorrel et al., 2012). This first inner island (Fig. 8) was colonized during the Proto-historic period (2600–2500 yr BP) as evidenced by the outpost sites of Huelva and the new for the time fluvio-marine harbour settlement of Aljaraque (Fig. 4).

The chenier plains grew progressively up-estuary by constant accumulation of tempestite beds, allowing for the full emergence of La Cascajera barrier in the 1st–2nd centuries CE (Fig. 8). Simultaneously, the large sand spits of Punta Umbría and Punta Arenilla grew seawards, migrating the estuary mouth towards the S, creating wide extensions of salt marshes. At Punta Umbría spit, coastal and salt-fish plants have also been found (La Peguera and El Eucaliptal). These settlements, that were established during the beginning of the first century CE, are progressively abandoned as the spit grows and fills the estuary shores; first La Peguera (1st to 2nd century CE) as it is located north and immediately after El Eucaliptal (2nd to 6th century CE), quasi-contemporary to La Cascajera (4th to 5th centuries CE) (Figs. 4 and 8). Thus, new landscapes were occupied by coastal settlements during the first century CE. At the end of the Roman period, from the 5th century CE on, the present configuration of the estuary was established and the later human settlements did not seem to be related with its morpho-dynamic evolutionary pattern (Fig. 8). In summary, the Holocene geomorphological evolution of the Tinto-Odiel estuary the creation and expansion of port areas (e.g. Onoba) and a set of salting fish factories (e.g. La Peguera, El Eucaliptal, La Cascajera) that depended on them (Campos et al., 2015).

## 6. Conclusions

The multidisciplinary analysis of Late Holocene sediments from La Cascajera (Saltés Island, Tinto-Odiel Estuary, SW Spain) provides a regressive sequence from a basal sandy tidal flat to a subrecent marshland. This sequence includes three intermediate phases (muddy tidal flat, chenier and washover fans) with a modelled  $^{14}\text{C}$  age ranging from the late first century BCE to the early second century CE. The textural and palaeontological features of these high-energy facies indicate an erosion of the adjacent infralittoral bottoms and the nearby tidal channels, as well as from the cheniers on which they are deposited.

Once Saltés Island's sand barriers emerged and stabilized, they were occupied by human settlements. At La Cascajera, an industrial Roman settlement has been found related with the processing of marine resources (*cetariae*), since about the middle 4th century over the entire 5th century CE, i.e., approximately 250 years after the natural stabilization. This correlation between the geological record and the human settlements can be followed during almost 3000 years, with the development of new ports (e.g. *Onoba*) and salting fish factories (El Almendral, El Eucaliptal, La Cascajera, La Peguera) on the geomorphological units (sandy spits, cheniers, washover fans, marshlands) that were gradually emerging.

### Declarations of interest

None.

### Acknowledgements

We are very grateful to CEIMAR-Huelva International Excellence Campus and CIPHEN-Centro de Investigación en Patrimonio Histórico, Cultural y Natural of the Huelva University for its support and infrastructure. It is a contribution to the Patrimonio Project CEI-Patrimonio 2014 (Marismas del Odiel-PatrimoniUN10).

### Funding

This work was funded by the Spanish Ministry of Economy and Competitiveness [MICINN-FEDER I + D Project CGL2010-15810/BTE]; the European Union [EU-Excellence Project of the Andalusia Board SEJ-4770]; a Chilean DIUDA Project [no. 15/10] and supported by three Research Groups of the Andalusia Board [RNM-238, RNM-293 and RNM-349].

### References

- Alonso, C., Menanteau, L., Gracia, F.J., Ojeda, R., 2007. Gearqueología y paleomorfología litoral de la ensenada de Bolonia: primeros resultados y nuevas propuestas. In: Arévalo, A., Bernal, D. (Eds.), Las “Cetariae” de “Baelo Claudia”: avance de las investigaciones arqueológicas en el barrio meridional (2000–2004). Universidad de Cádiz, Consejería de Cultura, Junta de Andalucía, pp. 521–538.
- Alonso, C., Gracia, F.J., Benavente, J., 2009. Evolución histórica del sector meridional de la Bahía Interna de Cádiz. RAMPAS 11, 13–37.
- Augustinus, P., 1989. Cheniers and chenier plains: a general introduction. Mar. Geol. 90, 219–229.
- Barahona, E., 1974. Arcillas de ladrillería de la provincia de Granada: evaluación de algunos ensayos de materias primas. Universidad de Granada, Spain (Ph. D. Thesis).
- Bazzana, A., Bedia, J., 2005. Excavaciones en la Isla de Saltés (Huelva) 1988–2001. Consejería de Cultura, Junta de Andalucía (717 pp.).
- Bermejo, J., Campos, J.M., García Rincón, J.M., Vera, J.C., 2016. Arqueología en el paraje natural de Marismas del Odiel (Huelva) y su entorno, desde la prehistoria hasta época tardoantigua. In: Campos, J.M. (Ed.), El Patrimonio Histórico y Cultural en el paraje natural Marismas del Odiel: Un enfoque diacrónico y transdisciplinar. Universidad de Huelva, Puerto de Huelva, pp. 107–129.
- Borrego, J., 1992. Sedimentología del estuario del río Odiel (Huelva, S.O. España). Universidad de Sevilla, Spain (Ph. D. Thesis).
- Borrego, J., Morales, J.A., Pendón, J.G., 1993. Holocene filling of an estuarine lagoon along the mesotidal coast of Huelva: the Piedras River mouth, southwestern Spain. J. Coast. Res. 8, 321–343.
- Borrego, J., Ruiz, F., Gonzalez-Regalado, M.L., Pendón, J.G., Morales, J.A., 1999. The Holocene transgression into the estuarine central basin of the Odiel River mouth

- (Cadiz gulf, SW Spain): lithology and faunal assemblages. *Quat. Sci. Rev.* 18, 769–788.
- Borrego, J., Morales, J.A., Gil, N., 2000. Facies deposicionales y evolución reciente de una llanura de cheniers en la desembocadura de la Ría de Huelva (S. O. España). *Rev. Soc. Geol. Esp.* 13 (3–4), 405–416.
- Borrego, J., López González, N., Carro, B., 2004. Geochemical signature as palaeoenvironmental markers in Holocene sediments of the Tinto River estuary (Southwestern Spain). *Estuar. Coast. Shelf Sci.* 61, 631–641.
- Bronk Ramsey, C., 2001. Development of the radiocarbon calibration program OxCal. *Radiocarbon* 43 (2A), 355–363.
- Bronk Ramsey, C., 2008. Deposition models for chronological records. *Quat. Sci. Rev.* 27 (1–2), 42–60.
- Bronk Ramsey, C., 2009. Bayesian analysis of radiocarbon dates. *Radiocarbon* 51 (1), 337–360.
- Bronk Ramsey, C., 2012. *Oxcal 4.1 manual. Web interface build number: 69.* [http://c14.arch.ox.ac.uk/oxcalhelp/hlp\\_contents.html](http://c14.arch.ox.ac.uk/oxcalhelp/hlp_contents.html) (last updated: 20/4/2012).
- Bronk Ramsey, C., Allen, M.J., 1995. Analysis of the radiocarbon dates and their archaeological significance. In: Cleal, R.M.J., Walker, K.E., Montague, R. (Eds.), *Stonehenge in Its Landscape: Twentieth Century Excavations.* English Heritage, London, pp. 526–535.
- Buck, C.E., Kenworthy, J.B., Litton, C.D., Smith, A.F.M., 1991. Combining archaeological and radiocarbon information - a Bayesian-approach to calibration. *Antiquity* 65 (249), 808–821.
- Buck, C.E., Litton, C.D., Smith, A.F.M., 1992. Calibration of radiocarbon results pertaining to related archaeological events. *J. Archaeol. Sci.* 19 (5), 497–512.
- Campos, J.M., Pérez, J.A., Vidal, N.O., 1999. Las cetariae del litoral onubense en época romana. Servicio de Publicaciones de la Universidad de Huelva, Spain.
- Campos, J.M., Pérez, J.A., Vidal, N.O., Gómez, A., 2002. Las industrias de salazones del litoral onubense: Los casos del Eucaliptal (Punta Umbría) y Cerro del Trigo (Almonte). In: *Huelva en su historia 2ª época* 9, pp. 76–96.
- Campos, J.C., Rodríguez-Vidal, J., Bermejo, J., González-Regalado, M.L., Abad, M., Cáceres, L.M., Ruiz, F., Toscano, A., Clemente, M.J., Gómez, P., Fernández Sutilo, L., Toscano Pérez, C., Robles Esparcia, S., 2014. Nuevos estudios arqueológicos y geomorfológicos en el Paraje Natural de Marismas del Odiel: La barrera arenosa de La Cascajera. In: 1ª Jornadas Internacionales Marismas del Odiel: Reserva de la Biosfera, Huelva.
- Campos, J.C., Bermejo, J., Rodríguez-Vidal, J., 2015. La ocupación del litoral onubense en época romana y su relación con eventos marinos de alta energía. *Geomorfol.* 29 (1–2), 75–93.
- CEEPYC (Centro de Estudios y Experimentación de Puertos y Costas), 1990. Plan de estudio de la dinámica litoral de la Provincia de Huelva. Technical Report. Dirección General de Puertos y Costas, Madrid, Spain.
- Cuena, G.J., 1991. Proyecto de regeneración de las playas de Isla Cristina. In: *Memorias del Ministerio de Obras Públicas y Transporte.* Technical Report (Huelva, Spain).
- Dabrio, C.J., Zazo, C., Goy, J.L., Sierro, F.J., Borja, F., Lario, J., González, J.A., Flores, J.A., 2000. Depositional history of estuarine infill during the Late Pleistocene-Holocene postglacial transgression. *Mar. Geol.* 162, 381–404.
- Domínguez-Delmas, M., Alejano-Monge, R., Van Daalen, S., Rodríguez-Trobajo, E., García-Gonzalez, I., Susperregi, J., Wazny, T., Jansma, E., 2015. Tree-rings, forest history and cultural heritage: current state and future prospects of dendroarchaeology in the Iberian Peninsula. *J. Archaeol.* 57, 180–196.
- Fernández Caliani, J.C., Ruiz, F., Galán, E., 1997. Clay mineral and heavy metal distribution in the lower estuary of Huelva and adjacent Atlantic shelf, SW Spain. *Sci. Total Environ.* 198, 181–200.
- Font, E., Veiga-Pires, C., Pozo, M., et al., 2013. Benchmarks and sedimentary source(s) of the 1755 Lisbon tsunami deposit at Boca do Rio Estuary. *Mar. Geol.* 343, 1–14.
- García Rincón, J.M., Rodríguez-Vidal, J., 1990. El sondeo estratigráfico de La Glorieta (Punta Umbría, Huelva). *Huelva Arqueológica* 12, 380–399.
- Gofas, S., Moreno, D., Salas, C. (Eds.), 2011. *Moluscos marinos de Andalucía. Vol I and Vol. II.* Servicio de Publicaciones e Intercambio Científico, Universidad de Málaga, Spain.
- Gómez Álvarez, G., 2013. Guía de las conchas marinas de Huelva. Diputación de Huelva, Spain.
- Gómez Toscano, F., Campos Carrasco, J.M., 2001. *Arqueología en la ciudad de Huelva (1966–2000).* Universidad de Huelva (273 pp.).
- González-Regalado, M.L., Ruiz, F., Baceta, J.L., Pendón, J.G., Abad, M., Hernández-Molina, F.J., Somoza, L., Díaz del Río, V., 2000. Foraminíferos bentónicos actuales de la plataforma continental del norte del Golfo de Cádiz. *Geogaceta* 29, 75–79.
- González-Regalado, M.L., Ruiz, F., Baceta, J.L., González-Regalado, E., Muñoz, J.M., 2001. Total benthic foraminifera assemblages in the southwestern Spanish estuaries. *Geobios* 34, 39–51.
- Goy, J.L., Zazo, C., Dabrio, C.J., Borja, F., Sierro, F.J., Flores, J.A., 1996. Global and regional factors controlling changes of coastlines in southern Iberia (Spain) during the Holocene. *Quat. Sci. Rev.* 15, 773–780.
- Goy, J.L., Zazo, C., Dabrio, C.J., 2003. A beach-ridge progradation complex reflecting periodical sea-level and climate variability during the Holocene (Gulf of Almería, Western Mediterranean). *Geomorphology* 50, 251–268.
- Grützner, C., Reicherter, K., Hübscher, C., Silva, P.G., 2012. Active faulting and neotectonics in the Baelo Claudia area, Campo de Gibraltar (southern Spain). *Tectonophysics* 554–557, 127–142.
- Gulbrandsen, R.A., 1960. Petrology of the Meade Peak phosphate shale member of the Phosphoria Formation at coal Canyon, Wyoming. *U.S. Geol. Surv. Bull.* 1111-C, 71–146.
- Junta de Andalucía, 1993. Atlas de los recursos marinos del golfo de Cádiz. In: *Litoral de Huelva.* Junta de Andalucía, Spain.
- Lario, J., 1996. Último y Presente Inter-glacial en el área de conexión Atlántico-Mediterráneo: Variaciones del nivel del mar, paleoclima y paleoambientes. Universidad Complutense de Madrid, Spain (Ph.D. Thesis).
- Leblanc, M., Morales, J.A., Borrego, J., Elbaz-Poulichet, F., 2000. 4,500 year old mining pollution in southwestern Spain: long-term implications for modern mining pollution. *Econ. Geol.* 95, 655–662.
- M.O.P.U. (Ministerio de Obras Públicas y Urbanismo), 1991. Estudio sobre el oleaje para la primera fase del estudio de evolución de la playa de Castilla (Huelva). Technical Report (Madrid, Spain).
- Martín de la Cruz, J.C., 1998. El poblamiento Pre y Protohistórico de Aljaraque. Huelva. In: *Homenaje a Jose María Blázquez Vol. 1.* pp. 217–242 (Mangas Manjarrés, J.; Alvar Ezquerro, J. (Coord.)).
- Martins, J.M.M., Soares, A.M.M., 2013. Marine radiocarbon reservoir effect in Southern Atlantic Iberian coast. *Radiocarbon* 55 (2–3), 1123–1134.
- Morales, J.A., 1997. Evolution and facies architecture of the mesotidal Guadiana River delta (S.W. Spain, Portugal). *Mar. Geol.* 138, 127–148.
- Morales, J.A., Borrego, J., Ballesta, M., 2004. Influence of harbour constructions on morphosedimentary changes in the Tinto-Odiel estuary mouth (south-west Spain). *Environ. Geol.* 46, 151–164.
- Morales, J.A., Borrego, J., San Miguel, E.G., López-González, N., Carro, B., 2008. Sedimentary record of recent tsunamis in the Huelva Estuary (southwestern Spain). *Quat. Sci. Rev.* 27, 734–746.
- Morales, J.A., Borrego, J., Davis Jr., R.A., 2014. A new mechanism for chenier development and a facies model of the Saltés Island chenier plain (SW Spain). *Geomorphology* 204, 265–276.
- Oliás, M., Nieto, J.M., 2015. Background conditions and mining pollution throughout history in the Río Tinto (SW Spain). *Environmen* 2, 295–316.
- Otvos, E.G., 2000. Beach ridges-definitions and significance. *Geomorphology* 32, 83–108.
- Pérez Quintero, J.C., 1989. Introducción a los moluscos onubenses. I: Faunística. Agencia de Medio Ambiente, Junta de Andalucía, Sevilla, Spain.
- Reimer, P.J., Bard, E., Bayliss, A., Beck, J.W., Blackwell, P.G., Bronk Ramsey, C., Grootes, P.M., Guilderson, T.P., Hafliðason, H., Hajdas, I., Hatte, C., Heaton, T.J., Hoffmann, D.L., Hogg, A.G., Hughen, K.A., Kaiser, K.F., Kromer, B., Manning, S.W., Niu, M., Reimer, R.W., Richards, D.A., Scott, E.M., Southon, J.R., Staff, R.A., Turney, C.S.M., van der Plicht, J., 2013. IntCal13 and Marine13 radiocarbon age calibration curves 0–50,000 years cal BP. *Radiocarbon* 55, 1869–1887.
- Requena, A.A., Clauss, F.L., Fernández Caliani, J.C., 1991. Mineralogía y aspectos geoquímicos de los sedimentos actuales del río Odiel (Huelva). Cuaderno del Laboratorio Xeológico de Laxe 16, 135–144.
- Rodríguez-Ramírez, A., Rodríguez-Vidal, J., Cáceres, L.M., Clemente, L., Belloumini, G., Manfra, L., Improta, S., De Andrés, J.R., 1996. Recent coastal evolution of the Doñana National Park (SW Spain). *Quat. Sci. Rev.* 15, 803–809.
- Rodríguez-Ramírez, A., Cáceres, L.M., Rodríguez-Vidal, J., 2000. Dinámica y evolución de flechas litorales: El litoral onubense (SO, España). In: De Andrés, J.R., Gracia, F.J. (Eds.), *Geomorfología litoral. Procesos Activos.* Instituto Tecnológico y Geominero de España, Ministerio de Ciencia y Tecnología, Madrid, pp. 101–113.
- Rodríguez-Vidal, J., 1987. Modelo de evolución geomorfológica de la flecha litoral de Punta Umbría, Huelva, España. *Cuat. Geomorfol.* 1, 247–256.
- Rodríguez-Vidal, J., Ruiz, F., Cáceres, L.M., Abad, M., González-Regalado, M.L., Pozo, M., Carretero, M.I., Monge, A.M., Gómez, F., 2011. Geomarkers of the 218–209 BC Atlantic tsunamis in the Roman Lacus Ligustinus (SW Spain): a palaeogeographical approach. *Quat. Int.* 242, 201–212.
- Rodríguez-Vidal, J., Abad, M., Cáceres, L.M., González-Regalado, M.L., Clemente, M.J., Ruiz, F., Izquierdo, T., Toscano, A., Gómez, P., Campos, J., Bermejo, J., Martínez-Aguirre, A., 2014. Relleno morfosedimentario y poblamiento humano del estuario de los ríos Tinto y Odiel (Huelva) durante la segunda mitad del Holoceno. In: Schanbel, S., Gómez Gutiérrez, A. (Eds.), *Avances de la Geomorfología en España 2012–2014.* Sociedad Española de Geomorfología y Universidad de Extremadura, Cáceres, pp. 604–607.
- Rodríguez-Vidal, J., Campos Carrasco, J., Cáceres Puro, L.M., 2015. Eventos marinos y asentamientos costeros en el suroeste de Iberia. *Cuat. Geomorfol.* 29 (1–2), 5–18.
- Ruiz, F., 2001. Trace metals in estuarine sediments from the southwestern Spanish coast. *Mar. Pollut. Bull.* 42, 482–490.
- Ruiz, F., Abad, M., Rodríguez-Ramírez, A., Cáceres, L.M., Rodríguez Vidal, J., Pino, R., Muñoz, J.M., 2005a. A statistical approach to the critical storm period analysis. In: Lehr, J. (Ed.), *The Water Encyclopedia.* John Wiley & Sons, New York, pp. 1–5.
- Ruiz, F., Rodríguez-Ramírez, A., Cáceres, L.M., Rodríguez-Vidal, J., Carretero, M.I., Abad, M., Oliás, M., Pozo, M., 2005b. Evidence of high-energy events in the geological record: Mid-Holocene evolution of the southwestern Doñana National Park (SW Spain). *Palaeogeogr. Palaeoclimatol. Palaeoecol.* 229, 212–229.
- Ruiz, F., Abad, M., Rodríguez-Vidal, J., Cáceres, L.M., González-Regalado, M.L., Carretero, M.I., Pozo, M., Gómez, F., 2008. The geological record of the oldest historical tsunamis in southwestern Spain. *Rev. Ital. Paleontol. Stratigr.* 204, 47–64.
- Ruiz, F., Rodríguez-Vidal, J., Abad, M., Cáceres, L.M., Carretero, M.I., Pozo, M., Rodríguez-Llanes, J.M., Gómez-Toscano, F., Izquierdo, T., Font, E., Toscano, A., 2013. Sedimentological and geomorphological imprints of Holocene tsunamis in southwestern Spain: an approach to establish the recurrence period. *Geomorphology* 203, 97–104.
- Schneider, H., Höfer, D., Trog, C., Mäusbacher, R., 2016. Holocene landscape development along the Portuguese Algarve coast – a high resolution palynological approach. *Quat. Int.* 407, 47–63.
- Schultz, L.G., 1964. Quantitative interpretation of mineralogical composition from x-ray and chemical data for the Pierre Shale. *Geol. Surv. Prof. Pap.* 391, 1–31.
- Selby, K.A., Smith, D.E., 2007. Late Devensian and Holocene sea-level changes on the Isle of Skye, Scotland, UK. *J. Quat. Sci.* 22, 119–139.
- Silva, P.G., Reicherter, K., Grützner, C., Bardaji, T., Lario, J., Goy, J.L., Zazo, C., Becker-Heidmann, P., 2009. Surface and subsurface paleoseismic records at the ancient



- Roman city of Baelo Claudia and the Bolonia Bay area, Cádiz (South Spain). *J. Geol. Soc. Lond. Spec. Publ.* 316, 93–121.
- Sorrel, P., Debret, M., Billeaud, I., Jaccard, S.L., McManus, J.F., Tessier, B., 2012. Persistent non-solar forcing of Holocene storm dynamics in coastal sedimentary archives. *Nat. Geosci.* 5, 892–896.
- Stuiver, M., Polach, H.A., 1977. Discussion: reporting of  $^{14}\text{C}$  data. *Radiocarbon* 19 (3), 355–363.
- Stuiver, M., Pearson, G.W., Braziunas, T., 1986. Radiocarbon age calibration of marine samples back to 9000 cal yr BP. *Radiocarbon* 28 (2B), 980–1021.
- Vanne, J.R., 1970. L'hydrologie du Bas Guadalquivir. CSIC-Consejo Superior de Investigaciones Científicas, Madrid.
- Vilanova, I., Prieto, A.R., Espinosa, M., 2006. Palaeoenvironmental evolution and sea-level fluctuations along the southeastern Pampa grasslands coast of Argentina during the Holocene. *J. Quat. Sci.* 21, 227–242.
- Zazo, C., Goy, J.L., Somoza, L., Dabrio, C.J., Belluomini, G., Improta, S., Lario, J., Bardají, T., Silva, P.G., 1994. Holocene sequence of relative sea level highstand lowstand in relation to the climatic trends in the Atlantic–Mediterranean linkage coast: forecast for future coastal changes and hazards. *J. Coast. Res.* 10 (4), 933–945.
- Zazo, C., Dabrio, C.J., Goy, J.L., Lario, J., Cabero, A., Silva, P.G., Bardají, T., Mercier, N., Borja, F., Roquero, E., 2008. The coastal archives of the last 15 ka in the Atlantic–Mediterranean Spanish linkage area: sea level and climatic changes. *Quat. Int.* 181, 72–87.